Molecular BioSystems

Accepted Manuscript

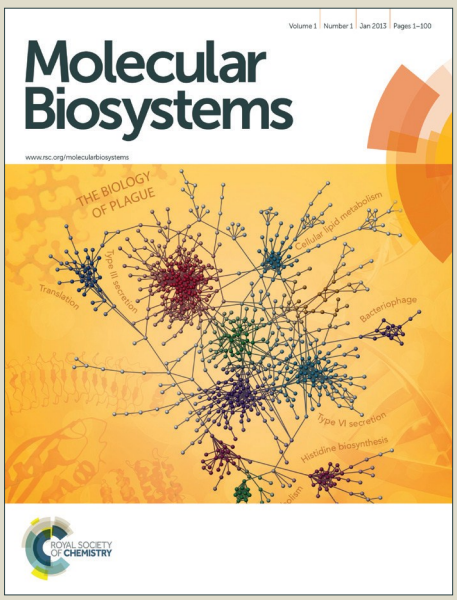

ROYAL SOCIETY OF CHEMISTRY

www.rsc.org/molecularbiosystems

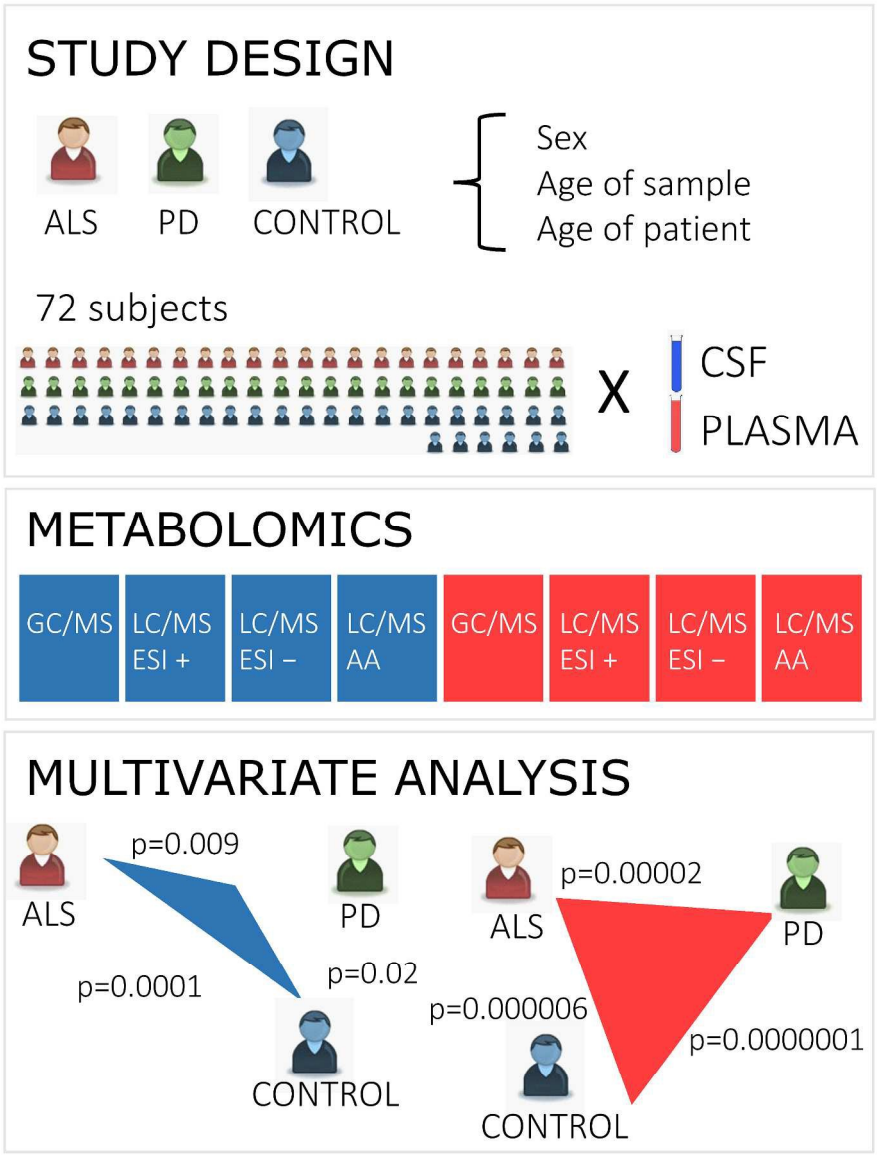

240x310mm (300 x 300 DPI)

Multi–platform Mass Spectrometry Analysis of the CSF and Plasma Metabolomes of Rigorously Matched Amyotrophic Lateral Sclerosis, Parkinson's Disease and Control Subjects

Anna Wuolikainen[a*], Pär Jonsson[a], Maria Ahnlund[b], Henrik Antti[a], Stefan L. Marklund[c], Thomas Moritz[b], Lars Forsgren[d], Peter M Andersen[d], Miles Trupp[d].

[a]Department of Chemistry, Umeå University, SE 901 85, Sweden. [b]Umeå Plant Science Centre, Department of Forest Genetics and Plant Physiology, Swedish University of Agricultural Sciences, SE 901 83 Umeå, Sweden, [c]Department of Medical Biosciences, Clinical Chemistry, Umeå University, Umeå, SE 901 85, Sweden. [d]Department of Pharmacology and Clinical Neuroscience, Umeå University, Umeå, SE 901 85, Sweden.

*Corresponding author

Anna Wuolikainen
Department of Chemistry
Umeå University, SE 901 85, Sweden.
anna.wuolikainen@umu.se

Abstract

Amyotrophic lateral sclerosis (ALS) and Parkinson's disease (PD) are protein-aggregation diseases that lack clear molecular etiologies. Biomarkers could aid in diagnosis, prognosis, planning of care, drug target identification and stratification of patients into clinical trials. We sought to characterize shared and unique metabolite perturbations between ALS and PD and matched controls selected from patients with other diagnoses, including differential diagnoses to ALS or PD that visited our clinic for a lumbar puncture. Cerebrospinal fluid (CSF) and plasma from rigorously age-, sex- and sampling-date matched patients were analyzed on multiple platforms using gas chromatography (GC) and liquid chromatography (LC)-mass spectrometry (MS). We applied constrained randomization of run orders and orthogonal partial least squares projection to latent structures-effect projections (OPLS-EP) to capitalize upon the study design. The combined platforms identified 144 CSF and 196 plasma metabolites with diverse molecular properties. Creatine was found increased and creatinine decreased in CSF of ALS patients compared to matched controls. Glucose was increased in CSF of ALS patients and α-hydroxybutyrate was increased in CSF and plasma of ALS patients compared to matched controls, indicating altered glutathione metabolism. Leucine, isoleucine and ketoleucine were increased in CSF of both ALS and PD. Together, these studies, in conjunction with earlier studies, suggest alterations in energy utilization pathways and have identified and further validated perturbed metabolites to be used in panels of biomarkers for diagnosis of ALS and PD.

Key words: Amyotrophic lateral sclerosis (ALS), Parkinson's disease (PD), cerebrospinal fluid (CSF), plasma, mass spectrometry (MS), metabolomics.

Introduction

There is currently no established fluid biomarker in routine use for diagnosing amyotrophic lateral sclerosis (ALS) or Parkinson's disease (PD). Though there are guidelines or recommendations, there is at present no consensus on which procedures, including cerebrospinal fluid (CSF) analysis, to perform/not perform when investigating new cases. At our department, collecting and analysis of CSF are included in the routine investigation for a variety of neurodegenerative conditions. ALS and PD are diagnosed by clinical examination and exclusion of other diseases, and are more precisely diagnosed when the disease has progressed. Blood relatives of patients with ALS or PD have a slight increased risk of developing the same disease[1] and overall also have an increased incidence for other neurodegenerative syndromes[2]. This is best depicted within the ALS syndrome where pleiotropy, including for parkinsonism, has been demonstrated for several of the 30 genes now known to cause ALS[3]. The emerging evidence is that there is considerable overlap in predisposing genetic etiology and pathomechanisms between several neurodegenerative disorders.

While neurodegenerative disorders such as ALS and PD exhibit heterogeneous genetic causes and disease courses, many share a molecular pathology of misfolding and aggregation of disease specific proteins[4-5]. Recent efforts have focused upon identifying underlying molecular etiologies leading to deficits in protein homeostasis and autophagy[6-7]. Metabolic patterns have emerged, indicating that mitochondrial function and management of oxidative stress are critical for maintaining protein homeostasis[8]. Since mitochondrial function is critically sensitive to metabolic alterations, small but chronic changes in metabolic signatures may increase the likelihood of mitochondrial mediated oxidative stress and lipid modifications causing lysosomal and autophagy failure leading to protein misfolding, formation of fibrils and aggregation[9].

The considerable heterogeneity in the predisposing genetic causes of ALS and PD appeals the investigation of mechanisms closer to the final pathology—protein aggregation leading to neuronal degeneration.

The first report of metabolomics in motor neuron disease performed on human subjects was published in 2005[10]. Metabolomics approaches to investigate systems biology are increasingly popular due to the unique ability to reveal the combined environmental, genetic and physiological components leading to pathological states. Metabolomics can be used for screening of perturbed metabolic pathways of diseases for which pathological mechanisms may be unknown or poorly understood, to generate new data-driven hypotheses, or for validation of established hypotheses from genes, transcripts or proteins[11-13]. Since there is no single analytical method that can provide a complete coverage of the metabolome[14], complementary techniques increase the metabolite coverage and expand the number of metabolic pathways studied.

For the first time we report metabolomics results from CSF and plasma collected at the same visit to the hospital from ALS and PD patients. In this study we utilized multiple mass spectrometry (MS) platforms to investigate common and specific perturbations in the metabolome between ALS and PD, extending the comparisons towards a control

group to assessing the other disease as a second diseased control group. We applied a purpose developed data analytical approach[15] to minimize the influence of instrumental drift that could bias comparisons, by capitalizing upon the power of rigorously matched samples. Apart from screening for new potential candidate markers, we sought to verify candidate biomarkers identified in previous reports.

Materials and Methods

The study was performed in accordance with the Declaration of Helsinki[16] and approved by the Swedish medical ethical review board. Written informed consent was obtained from all patients.

Study design, selection of patients and samples

At the Department of Neurology at Umeå University Hospital, CSF and plasma samples are collected from non-fasting patients with various neurological conditions and kept in −80° freezers[17]. Since age of the test subject, storage time of the sample[18], sex of the patient, as well as a correct diagnosis are essential when performing metabolomic studies, we first selected a group of 22 ALS patients (16 males, 6 females) that was rigorously matched for age, sex and storage time, to a similar group of 22 (15 males, 7 females) patients with PD (1 female ALS patient was reclassified to male, hence 16 ALS males and 6 ALS females). The patients were only included if both plasma and CSF were available and had been collected at the same visit. Having identified these 22 + 22 groups, we then searched the biobank for patients with other neurological conditions that matched the ALS and PD groups for age, sex and storage time. The aim was to create the control group as a sample of patients coming to the clinic, who may share early signs and symptoms with ALS or PD, and hence be candidates for a diagnostic test. We further aimed to target sporadic ALS cases without pre-knowledge about genetic background at the time of inclusion in the study, at a span in age where most sporadic patients are known to present with ALS. Since PD patients often presents at older age, the study was extended to include older ALS patients. With this approach we identified 28 control subjects (19 males, 9 females), 22 of them matching the ALS and PD patients on a 1:1:1 basis, however for 6 ALS and 6 PD patients two control individuals were found and matched (1:1:2).

A strict requirement was that the diagnosis of the included patients should be definite. For samples collected at the initial visit to our hospital with the diagnosis still uncertain, only patients for whom the initial or later investigations made the diagnosis certain were included. The included ALS patients were clinically investigated according to the revised European Federation of Neurological Societies (EFNS) Consensus Guidelines for Managing ALS[19] and the PD patients according to the United Kingdom Parkinson's Disease Society Brain Bank (UK PDSBB) criteria. In total, 72 matched patients passed all criteria and were included in the study (22 ALS, 22 PD and 28 control individuals) as summarized in Table S1. Patients were annotated with match number, sample biobank number, diagnosis, sex, age of patient at sampling and age of sample.

Sample preparation

CSF and plasma samples were extracted according to a standardized protocol[20]. 100 µL of plasma or CSF were aliquoted and added to 900 µL extraction solution consisting of methanol:water (8:1). The extraction solution was spiked with isotope labeled internal standards (500 ng/µl stocks of [$^{2}H_{4}$] succinic acid, [$^{13}C_{12}$] sucrose, [$^{13}C_{5}$,^{15}N] glutamic acid, cholesterol, [1,2,3-$^{13}C_{3}$] myristic acid, [$^{13}C_{4}$] palmitic acid and [$^{2}H_{6}$] salicylic acid) for gas chromatography (GC)/MS to a final concentration of 3.65 ng/µL in the plasma extracts while the CSF extracts were prepared to 4.5 ng/µL to compensate for different dilution effects during sample derivatization. Val-Tyr-Val, Leu-Enk, sulfadimethoxine, reserpine were added as internal standard for liquid chromatography (LC)/MS to a final concentration of 0.081 ng/µL in the CSF and plasma extracts. The extracts were split into 4 vials, to allow measurements with the multiple MS methods: GC/MS; LC/MS electrospray ionization (ESI) in both positive and negative mode (ESI+/−) and target amino acid analysis using LC/MS. Quality control samples were prepared by pooling CSF from a subset of subjects equally distributed between diagnoses (ALS, PD, controls) and plasma was pooled from all 72 subjects. To minimize confounding between metabolite variations related to disease with analytical drift, all run orders were randomized using constrained randomization[15], *i.e.* randomization was applied both between and within matched subjects. By applying this approach we were able to minimize the influence of the instrumental drift, except irregular drift (*i.e.* noise). Noise was instead handled by using the multivariate modelling approach, since only variability with structure are considered by the models.

Untargeted GC/MS

GC/MS requires volatile compounds for detection and this can be achieved by derivatization of metabolites. For derivatization, *o*-methylhydroxylamine hydrochloride 98% (Aldrich) (30 µL, 15 µg/µl) in pyridine was added to the samples, shaken with a MM301 beadmill (Retsch® GmbH & Co. KG) for 15 min, heated to 70 °C for 1 h and left for 16 h in room temperature. N-Methyl-*N*-trimethylsilyltrifluoroacetamide+1% trimethylchlorosilane (30 µL) were added to the samples, kept in room temperature for 1 h before heptane (30 µL, with 15 ng methylstearate/µL, injection standard) was added prior to GC/MS analysis. The same procedure was used for derivatization of metabolites in CSF but the amount of *O*-methylhydroxylamine hydrochloride (98%, 15 µg/µl in pyridine), N-Methyl-*N*-trimethylsilyltrifluoroacetamide +1% trimethylchlorosilaneand heptane (with 15 ng methylstearate/µL, injection standard) was lowered to 20 µL each. Nine quality control samples were distributed along the run order in the analysis of plasma samples, however for analysis of CSF samples, no quality control samples were analyzed by GC/MS. 1 µL aliquot was injected splitless by an CTC Combi Pal autosampler (CTC Analytics AG, Zwingen, Switzerland) into an Agilent 6890N gas chromatograph (Agilent Technologies, Santa Clara, CA, USA) equipped with a 10 m × 0.18 inner diameter fused-silica capillary column chemically bonded with 0.18 µm DB 5-MS stationary phase (J&W Scientific, Folsom, CA, USA). The injector temperature was set to 270 °C, the septum purge gas was turned on after 60 s at a flow rate of 20 mL/min. The initial

column temperature was 70°C and kept steady for 2 min. Temperature was increased by 40 °C/min until a temperature of 320 °C was reached. Stop temperature was kept for 2 min before the oven was allowed to return and stabilize at the initial temperature. The gas flow rate through the column was 1 mL/min. The column outlet was introduced into the ion source of a Pegasus III time of flight MS (Leco® Corp., St Joseph, MI, USA). The transfer line temperature was set to 250 °C and the ion source temperature was set to 200 °C. Ions were produced by a 70 eV electron beam (2.0 mA). Acceleration voltage was switched on after a 165 s solvent delay and masses were acquired between *m/z* 50-800, at a rate of 30 spectra/s for 445 s. Chromatographic profiles were extracted using in-house developed scripts.

Untargeted LC/MS

LC/MS was recorded using both ESI+ and ESI−. Chromatography was performed on an Agilent 1290 Infinity ultra-high pressure liquid chromatography system. 2 µL aliquot of the dissolved sample extract (in 50% methanol, correspond to 20 µl extracted sample) was injected onto a 2.1 x 100 mm, 1.7 µm Kinetex C_{18} ultra-high pressure liquid chromatography column (Phenomenex Inc, CA, USA) held at 40 °C. The column was eluted with a series of linear gradients: 1-20% B over 0-4 min, 20-40% B over 4-6 min, 40-95% B over 6-9 min, where A was 0.1% formic acid in water and B was acetonitrile:isopropanol (72:25 v/v) with 0.1% formic acid, flow rate 500 µl/min. Then the mobile phase was held at 95% B for 4.5 min, returned to 1% B at 14.50 min and kept at 1% B for a further 4.5 min before the next injection. The ultra-high pressure liquid chromatography was coupled to an Agilent G6540 quadrupole-time of flight tandem MS (Agilent Technologies, Santa Clara, CA, USA) equipped with a Dual Jet Stream ESI source, operating with 4.0kV capillary voltage in both positive and negative ion modes (sheath gas temperature 350 °C, sheath gas flow rate 11 L/min, drying gas temperature 300 °C, drying gas flow rate 8L/min and nebulizer pressure 40 psi in positive mode and 0 psi in negative mode). The fragmenter voltage was 100 V. All mass spectral data were acquired in centroid mode, 70-1700 m/z at a rate of 4 spectra/s. For internal calibration a reference solution of purine and HP-0921 was infused to the MS (positive ion mode: m/z 121.0509 and 922.0098; negative ion mode: m/z 119.0363 and 966.0007). Nine quality control samples were distributed along the runorder during each analysis. The run orders were randomized using constrained randomization[15]. Peaks were extracted using the MassHunter Qualitative Analysis B.05.00 software (Agilent Technologies, Santa Clara, CA, USA), by the Find Compound by Molecular Feature (MFE) algorithm. To get a collective peak list from all samples, the sample-individual peak lists were imported into Mass Profiler Professional B.02.00 program (Agilent Technologies) and sorted (*i.e.* peaks present in <3% of samples were removed and obvious background peaks were excluded). All peak areas were reintegrated in MassHunter Qualitative Analysis.

Targeted LC/MS of amino acids

For targeted amino acid analysis, amino acids were labelled with tags for detection (AccQ•Tag™, Waters, MA, USA) as specified in the manufacturer's instructions and norvaline (a non-endogenous amino acid) was used as a standard reference. A reference

mixture of 29 amino acids was analyzed to allow targeted detection of amino acids. Quality control samples were distributed along the run order (7 quality control samples were measured for CSF and 3 quality control samples were measured for plasma). The analysis was performed using a Waters Acquity UPLC system coupled to a Micromass LCT Premier mass spectrometer (Waters, Millford, MA, USA) operated in W-mode to detect the pre-tagged amino acids. The run orders were randomized using constrained randomization[15].

Identification and quality filtration of metabolite peaks

Metabolites detected by GC/MS were identified by means of chromatographic retention indices and comparison of the resolved mass spectra against the Umeå Plant Science Centre mass spectra library, public available mass spectra libraries (NIST 98 mass spectra library) and the mass spectra library hosted by the Max Planck Institute in Golm (http://csbdb.mpimp-golm.mpg.de/csbdb/gmd/gmd.html) or *de novo* identification via mass spectrum interpretation.

For metabolite peaks detected by LC/MS metabolite features were identified by exact mass determination and LC/MSMS spectra to the extent it was possible using open source libraries or databases (Metlin) or in-house standard databases at the Swedish Metabolomics Centre. Some non-identified peaks were classified, (*i.e.* phosphatidyl choline, lyso-phosphatidyl choline) and it should be noted that some of the peaks corresponded to compounds that are too hydrophobic for optimal measurements using this type of extraction. Tripeptides were classified and the amino acids in the tripeptides are listed; note, however, that the order of amino acids is not established. Unknowns were denoted by retention time, retention index and/or *m/z.* An in-house script was used for determination of peak area and identity of the targeted amino acids. The identity was assigned based on the measured standards and mass spectra comparisons.

To assess variability from extraction and analysis we calculated percentage relative standard deviation (%RSD) on the quality control samples. %RSD was used to determine by which analysis the metabolite was detected most robustly. The analysis generating the lowest %RSD for a metabolite, or the analysis providing the most certain identification of the metabolite, was used for data analysis. Peaks were discarded before data analysis if %RSD>40 or if poor analytical quality was detected manually (*i.e.* a high rate of missing values were found amongst the control, ALS and PD samples). Some amino acids measured by the untargeted methods showed low %RSD due to robust measurements as compared to the targeted LC/MS amino acid analysis and were hence used instead. The exception in CSF was glutamic acid (better measured with LC/MS ESI−) and exceptions in plasma were asparagine (LC/MS ESI−), glutamine (LC/MS ESI−), leucine (GC/MS), proline (GC/MS), threonine (GC/MS), tryptophan (GC/MS), tyrosine (LC/MS ESI+) and valine (GC/MS).

Data analysis

Metabolomics data from the individual platforms were overviewed using principal

component analysis[21] for visualization of variation in multiple variables. Before principal component analysis the data was mean centered and scaled to unit variance. Drift and possible outliers detected by the principal component analysis were investigated by inspection of internal standards and quality control samples. Data from the different platforms were combined for the subsequent analysis. A combination of identified and non-identified metabolites were evaluated for the discrimination between ALS, PD and controls.

Orthogonal partial least squares projections to latent structures (OPLS)[22] and OPLS-discriminant analysis (DA)[23] were used to consider variable correlations in the modelling of group mean differences between sample classes (ALS, PD and controls). The R2Y value represents the modeled class discrimination, ranging from 0 (no discrimination) to 1 (perfect discrimination). The Q2 represents the predicted class discrimination ranging from $-\infty$ to 1.

Since previous studies have demonstrated effects of sex, age of patient, age of sample and analytical drift on acquired metabolite profiles[18, 24-25], this study was designed to minimize these factors by defining a collection of rigorously matched sets of ALS, PD and controls. Table S1 shows the 22 groups of patients exhibiting very low mean standard errors in age of patient (0.8 years) and age of sample (2.1 months). To capitalize on the novel study design with rigorously matched patients and controls, a novel multivariate analysis method −orthogonal projection to latent structures-effect projections (OPLS-EP)[15] was used. OPLS-EP models of the effect changes (*e.g.* disease-control) were used to investigate common variable pattern (metabolite signature) for each matched pair and to compare the magnitude of change between the matched pairs. This can be regarded as a multivariate "paired" statistical test in latent variables. For each matched pair, a predicted response (Ypred) is calculated (the target value is 1) by OPLS-EP. If all pairs yield Ypred=1, the differences between the two classes is consistent amongst the pairs; deviations from 1 indicate inconsistency, where a value >1 indicates a positive difference (the pair is less similar) and value <1 indicates a negative difference (the pair is more similar). Wilcoxon's test was used to assess the univariate significance of each variable (metabolite) focusing between matched subjects. Significance level of the test was set to 95% (from here stated as 'significant according to univariate test').

First all variables were used in the OPLS-DA or the OPLS-EP model. ALS and PD were modelled versus matched controls and versus each other. Seven fold cross-validation was used to estimate the quality of the model and to establish a confidence interval around the model weights. For the six pairs assigned two matched controls, each control was used independently; and to avoid over-estimation of the model performance they were kept in the same cross-validation group. Metabolites were considered significant in a model when the Jack-knife confidence interval (95%) of the weight, computed from all rounds of cross validation, did not include the value zero. New models based on significant variables were calculated. R2Y, Q2 for all models can be found in Table S2. Disease profiles for each matched pair, compared to the mean metabolite disease profile

calculated from all 22 pairs was predicted in the cross-validated model. Individual predicted values (Ypredcv) correspond to the predicted metabolite disease profile of a patient compared to the matched control. The value reflects the similarity to the models estimated mean metabolite disease profile.

Results

General performance of the mass spectrometry methods

We performed four different analytical experiments on both CSF and plasma for a total of eight distinct measurements listed in Table 1. In CSF, by combining all analytical platforms, 600 peaks were measured across the patient samples. Among the 600 peaks, 144 unique metabolites were identified (metabolites identified on multiple platforms were counted once). The mean %RSD for the CSF metabolites was 15.6%. In plasma, 1233 potential metabolites were detected in total, of which, 188 unique metabolites were identified. The mean %RSD for the plasma metabolites was 18.9%. As expected, amino acids measured by the targeted amino acid method showed low %RSD as compared to the untargeted GC/MS and LC/MS screening; however exceptions were found of amino acids (listed in methods) that were more robustly measured by the untargeted analysis. The highest percentage of identified compounds compared to resolved peaks, were detected using GC/MS, due to more complete spectral databases for identification of metabolites. LC/MS ESI− detected the greatest number of identified metabolites in plasma, while the platform that resolved the most peaks in plasma counting non-identified peaks was LC/MS ESI+.

Multivariate analysis accounting for individual sample matching

OPLS-EP models used for targeting effects of variables (metabolites) between pairs were compared to the corresponding OPLS-DA models. The OPLS-EP models exhibited significant improvements in predictive ability (Table S2) compared to the corresponding OPLS-DA. As an example, the R2Y value for the OPLS-DA model separating between ALS and controls in CSF was 0.57 compared to 0.96 for the corresponding OPLS-EP. Similarly, the Q2 value for the OPLS-DA model separating between ALS and controls in CSF was −0.05 compared to 0.22 for OPLS-EP. By predicting values for CSF versus plasma for ALS or PD versus matched controls a patient overview could be plotted (Figure 1). Neither CSF, nor plasma models or the combination were able to completely distinguish all ALS patients from matched controls nor all PD from matched controls. The visualization allows interpretation of distribution of predictions amongst the individual matched pairs, such that values close to 1 corresponds to the mean disease profile and patients with values higher than 1 drives the model while patients with values below 1 shows less conformation with the model.

Metabolites differentiating ALS patients from matched controls

OPLS-EP models were calculated using both identified and unidentified metabolites, however only identified metabolites are listed in the summarized metabolite profiles (Figure 2). Model weights (w[1]) are shown for significant metabolites according to the

OPLS-EP model and the univariate test, between ALS and matched controls in CSF (Figure 2A; analysis method, %RSD and HMDB numbers for the metabolites are listed in Table S3). CSF metabolites that most positively correlated with the metabolite profile of ALS (*i.e.* interpreted as increased in ALS compared to the matched controls) were β-D-methylglucopyranoside (fold=1.33; p=0.003), carnitine (fold=1.25; p=0.001), decenedioic acid (fold=1.20; p=0.001), creatine (fold=1.15; p=0.001), α-hydroxy butyric acid (fold=1.27; p=9.04 $*10^{-5}$), ketoleucine (fold=1.16; p=0.015) and glucose (fold=1.10; p=0.015). CSF metabolites that most negatively correlated to the metabolite profile of ALS (*i.e.* interpreted as decreased in ALS compared to the matched controls) included uracil (fold=0.82; p=0.003), ribitol (fold=0.85; p=0.05), succinyladenosine (fold=0.83; p=0.015), creatinine (fold=0.91; p=0.03), arabitol (fold=0.85; p=0.05), xylitol (fold=0.85; p=0.05), acetylalanine (fold=0.88; p=0.015), xylose (fold=0.87; p=0.001) and pentonic acid-1,4-lactone (fold=0.87; p=0.015). Creatinine was lower in 17/28 ALS cases compared to the matched controls in CSF (13/28 in plasma) and creatine was higher in 20/28 ALS cases compared to matched controls. Creatinine is a product of creatine, we therefore compared the two by plotting creatinine towards creatine in CSF. The two metabolites could not distinguish ALS from controls, however a shift towards more creatine and less creatinine was apparent in the ALS patient group (plots can be found in Figure S1).

Many plasma metabolites positively correlated to the metabolite profile of ALS and were significant according to the univariate test. The top five positively correlated metabolites were indole, tryptophan, oxoquinoline, adenosine monophosphate (AMP) and proline (Figure 2B; analysis method, %RSD and HMDB numbers for the metabolites are listed in Table S4). The five metabolites in plasma most negatively correlated to the metabolite profile of ALS were ribonic acid, prostaglandin A2 (PGA2), homovanillic acid, hypoxanthine and cysteamine (Figure 2B; analysis method, %RSD and HMDB numbers for the metabolites are listed in Table S4).

Metabolites differentiating PD patients from matched controls

CSF metabolites most correlated in the OPLS-EP to the PD metabolite profile and significant according to the univariate test, were alanine (fold=1.20; p=0.001), sorbitol (fold=1.43; p=0.007), pyroglutamic acid (fold=1.10; p=0.02), galactitol (fold=1.26; p=0.003), mannitol (fold=1.32; p=0.015), threonine (fold=1.18; p=0.01), saccharic acid-1,4-lactone (fold=1.20; p=0.003), isoleucine (fold=1.24 ; p=0.003), ketoleucine (fold=1.15; p=0.003), benzoic acid (fold=1.14 ; p=0.015), glutamine (fold=1.07; p=0.05), ornithine (fold=1.19; p=0.024), glycerol-3-phosphate (fold=1.36; p=0.05), histidine (fold=1.15; p=0.006), octadecanol (fold=1.08; p=0.015) sorbose (fold=1.14; p=0.05)(Figure 3A; analysis method, %RSD and HMDB numbers for the metabolites are listed in Table S5).

The metabolite in CSF contributing with negative correlation in the OPLS-EP to the PD metabolite profile was tetracosanoic acid (fold=0.97; p=0.015) (Figure 3A; analysis method, %RSD and HMDB numbers for the metabolites are listed in Table S5). The top five plasma metabolites that were positively correlated in the OPLS-EP to the metabolite

profile of PD and significant according to the univariate test were a tripeptide (LysHisMet), maltotriose, aconitic acid, urate and cysteine (Figure 3B; analysis method, %RSD and HMDB numbers for the metabolites are listed in Table S6). The top five metabolites in plasma that were negatively correlated in the OPLS-EP with the metabolite profile of PD included phosphatidylcholine (36:4), arabinose, oxalate, pyruvate, and fumarate (Figure 3B; analysis method, %RSD and HMDB numbers for the metabolites are listed in Table S6).

Metabolites differentiating ALS from matched PD

OPLS-EP models of CSF (Figure 4A; analysis method, %RSD and HMDB numbers for the metabolites are listed in Table S7) and plasma (Figure 4B; analysis method, %RSD and HMDB numbers for the metabolites are listed in Table S8) between matched ALS and PD revealed 6 identified CSF metabolites that were significantly different between the two diseases and 12 identified metabolites significantly different in plasma. In CSF, the 6 metabolites found to be significantly altered between ALS and PD according to the univariate test include increased α-hydroxy butyric acid (fold=1.51; p=0.02) and β-hydroxy butyric acid (fold=1.28; p=0.05), carnitine (fold=1.18; p=0.04) and decreased ammonia (fold=0.92; p=0.05), inosine (fold=0.88; p=0.03) and uracil (fold=0.85; p=0.01). In plasma, the 12 metabolites found to be significantly altered between ALS and PD according to the univariate test include increased carnitine, α-hydroxy butyrate, lactate, O-phosphoethanol and xanthine. Conversely, dihydroxybenzoate, hippurate, taurine, hypoxanthine, erythronic acid, adenine, lyso-phosphatidylcholine (14:0) and pregnelone sulphate were found decreased in ALS versus matched PD or increased in PD versus matched ALS in plasma.

'Unique' metabolite perturbations between matched ALS, PD and controls

In addition to those separating ALS from matched controls and PD from matched controls, metabolites that further discriminated between ALS and PD were of particular interest as candidate diagnostic markers. Metabolites significantly different in CSF and plasma between matched ALS and PD were compared to the metabolites found significant between ALS and matched controls or PD and matched controls. α-hydroxy butyric acid, carnitine and uracil were significant metabolites between ALS and matched control and ALS and matched PD in CSF (Table 2). No metabolite was found significantly altered both between PD and matched control and PD and matched ALS in CSF. Hypoxanthine was the only univariate significant metabolite between ALS and matched control and ALS and matched PD in plasma (Table 2). No metabolite was found significantly altered both between PD and matched control and PD and matched ALS in plasma.

'Shared' perturbations in CSF and plasma of ALS and PD patients

Metabolites non-significantly different in CSF and plasma between matched ALS and PD were compared to the metabolites found significant between ALS and matched controls and PD and matched controls. Shared perturbations between ALS and PD were, galactitol, saccharic acid-1,4-lactone, isoleucine, ketoleucine, ornithine, and sorbitol

significantly increased in CSF of both ALS and PD patients, compared to the matched controls (Table 3). In plasma, indole and proline were found to be significantly increased in both ALS and PD compared to matched controls (Table 3).

Discussion

Metabolites can be changed by a large set of factors, such as disease, sex, age and nutrition. This reflects the high responsiveness in the metabolome that makes metabolomics data highly informative of state and change. Today many studies strive to enhance the theoretical statistical power by increasing the number of samples, however, biased factors cannot be managed by simply expanding the size of cohorts. Changes in non-disease related metabolic patterns, such as age of patient or sample can mask molecular changes caused by a disease. In this study we attempted to eliminate some of these potential confounders. Using a rigorous experimental design we were able to detect significant alterations of previously reported candidate metabolite biomarkers but also elucidate new potential metabolites in CSF and plasma that may be used in panels of candidate markers for ALS and PD or for understanding of molecular pathology of neurodegenerative processes.

While the potential of metabolite biomarkers that could diffuse out of compromised cells and signal neurodegeneration through disease specific signatures in CSF or plasma is very exciting, different metabolomics studies have identified a generally non-overlapping list of candidates. Hence, we start by focusing our discussion on candidate metabolites, and associated biochemical pathways, that have been detected as significantly altered in previously published studies.

Alzheimer's disease has been termed type 3 diabetes[26] and there is increasing evidence of metabolic overlap between type 2 diabetes and neurodegenerative diseases. Perturbations in glucose metabolism have been reported in several neurodegenerative disorders including ALS, PD, and dementia.[27-29]. Type 2 diabetes patients are more likely to develop PD and PD patients with glucose dysregulation are more likely to develop dementia[30]. Recently, exenatide, a diabetes medication, has shown promising results in a clinical trial measuring disease progression in PD[31]. ALS has been reported associated with hypermetabolism[32-34] and energy utilization was recently shown to be altered in ALS[35].

In this study, ALS patients showed increased levels of glucose in CSF. We have further detected an increase in CSF of hexose alcohols including sorbitol and galactitol in ALS, and sorbitol, galactitol and mannitol in PD. Together, this suggests that excess glucose beyond the capacity of glycolysis may be converted to sorbitol. The fact that α-hydroxy butyric acid was important in separating ALS from PD in the multivariate modelling of both CSF and plasma suggest that the ALS pathology could exhibit similarity to the pre-diabetic insulin phenotype suggestive of this biomarker[36]. The polyol pathway (or the sorbitol-aldose reductase pathway) has been suggested to be involved in diabetic neuropathy[37] and has been reported to be increased in CSF of patients with Alzheimer's disease[38]. In this study we detected a decrease in CSF xylose in ALS and in a previous study a decrease in CSF xylose and xylitol in PD patients[39]. The three pentols ribitol, arabitol and xylitol were found reduced in CSF of patients with ALS, which may further indicate an alteration in pentose metabolism. In general, in CSF of ALS patients we

detected a striking decrease in CSF levels of pentose related alcohols, and conversely an increase in hexoses and hexols. The alteration of glucose homeostasis in neurodegenerative diseases may effect shunting of hexoses through the pentose phosphate pathway, a major route for conversion of hexoses to pentoses and a critical pathway for production of reducing equivalents in the form of NADPH. We previously detected an increase in pyroglutamate (5-oxoproline) in a case control study of PD patients[39] and in this study pyroglutamate was found increased in CSF of PD patients. As pyroglutamate is an intermediate in the generation of NADPH from glutathione, this may indicate changes in this critical pathway in PD. However, we instead detected increased levels of the glutathione pathway degradation product α-hydroxy butyric acid, in CSF of ALS patients compared to controls and PD; potentially indicating increased activity of the glutathione pathway. α-hydroxy butyric acid was further increased in plasma of ALS patients and has also been reported increased in plasma of ALS patients in a previous metabolomics study of two different sets of patients[40]. α-hydroxy butyric acid, BCAAs and aromatic amino acids have been suggested as possible early plasma markers for insulin resistance [36,41]. We have detected a reduction in the levels of the pyrimidine nucleotide base uracil in CSF and the purine nucleotide base hypoxanthine in plasma from patients with ALS; and we detect a decrease of the ribonucleic acid (RNA) precursor inosine in CSF of ALS patients compared to PD. Combined with the significant decrease in pentose derivatives in CSF of ALS, this suggests a general deficit in RNA synthesis (for a schematic overview see Figure 5). This is particularly interesting considering the identification of mutations in RNA-housekeeping genes (TARDBP, FUS/TLS, TAF15, ANG) as a cause of ALS. The combination of RNA metabolism deficits described here may create a background on which variants in RNA processing genes may have a dramatic impact. In this study we have also detected a significant decrease in the CSF levels of succinyladenosine in patients with ALS. This compound is the dephosphorylated form of an intermediate (adenosylsuccinate) in the adenosine biosynthesis pathway generated from inosine-monophosphate by the adenylosuccinate synthetase (ADSS) enzymes. Recently, whole exosome sequencing has detected mutations in a muscle specific ADSS (ADSSL1) in adolescent onset distal myopathy[42]. In another recent report, adenylosuccinate has been shown to be an insulin secretagogue for pancreatic beta-islet cells–inducing the secretion of insulin following glucose stimulation[43]. Taken together, our results suggest that reduced levels of a purine metabolite in CSF is a candidate mechanism for altered energy usage in ALS. Further examples of altered energy usage is seen in the decreased levels of the ketone body β-hydroxybutyrate in PD compared to ALS.

We have previously reported decreased creatinine in a distinct set of CSF samples[24] and increased plasma creatine and decreased creatinine have been reported in metabolomics studies of other patient groups as well[40]. Here we reproduced the results and detected significantly increased levels of creatine and decreased levels of creatinine in CSF from patients with ALS. As ALS is a muscle wasting disease, increases in plasma of breakdown products from muscle such as amino acids and residual creatinine are anticipated, but the decrease in creatinine in CSF suggests an altered metabolism of creatine in the brain. A much larger proportion of cellular creatinine is produced from the non-enzymatic degradation of phosphocreatine than from creatine, suggesting that increases in creatine and decreases of creatinine in CSF may be surrogate markers for

reduced levels of central nervous system phosphocreatine. This deficit could be caused by an alteration in the function of the enzyme creatine kinase, levels of the creatine transporter or reduced availability of adenosine triphosphate. As phosphocreatine is critical for mitochondrial shuttling of adenosine triphosphate, such a deficit would drastically compromise ability of neurons to meet high energy demands. It is interesting to note that we detected an increase in plasma AMP in ALS. Since the use of creatine as an ALS medication has been extensively studied and failed in clinical trials[44], our analysis of creatine and creatinine in CSF suggest that therapeutically increasing creatine kinase activity may be a more effective strategy.

Recent metabolomics analysis of CSF revealed that metabolite derivatives of branched chain amino acids are important for separating ALS from healthy control samples[45]. In this study, we detected a pattern of BCAAs and their metabolites increased in CSF of both ALS and PD. We specifically detected increased levels of isoleucine and ketoleucine in CSF of patients with ALS and PD. BCAAs are critical for brain energy metabolism, regulation of protein degradation as well as maintenance of glutamate homeostasis. Up to 50% of all α-amino groups of glutamate and glutamine are derived from leucine [46]. Leucine enters the brain from the blood more rapidly than any other amino acid through the neutral amino acid transporter on astrocytes. BCAAs are metabolized in astrocytes into their cognate ketoacids, released and subsequently taken up by neurons. This serves as an important mechanism for neurons to buffer glutamate levels by converting ketoleucine back to leucine, consuming glutamate in the process. Our results suggest that disruption of BCAA homeostasis may have effects on neuronal solute transport and excitatory neurotransmitter function. Leucine is further a key amino acid regulator of the mechanistic target of rapamycin (mTOR) complex 1 (mTORC1) –the critical mediator of protein synthesis and degradation[47]. When leucine is plentiful mTORC1 is active and promotes protein translation and suppresses autophagy[48]. And as such, leucine levels function as a critical regulator of autophagy. Our results suggest that further analysis of BCAA metabolism in neurodegenerative diseases is warranted, and in particular investigation of the role of leucine metabolites in modification of mTORC1 induction of autophagy. We further found increased saccarhic acid 1,4 lactone in CSF of both ALS and PD may that may indicate a disruption in lysosomal processing in both diseases since it is known to inhibit the lysosomal beta-glucuronidase.

We detected increased tryptophan, formylkynurenine and indole in plasma of ALS patients compared to controls. Various metabolites of the kynurenine pathway have been suggested to be involved in numerous neurodegenerative diseases such as Alzheimer's disease, Huntington's disease, PD[49] and ALS[50]. Increased concentrations of 3-hydroxykynurenine have been detected in post-mortem putamen and substantia nigra of PD, suggesting a defect in the kynurenine pathway and production of reduced nicotinamide adenine dinucleotide (NADH)[51]. It was recently reported that up regulation of this pathway is one of the mechanisms mediating insulin resistance[52]. An observation from this study was that a combination of metabolites from the pathway was necessary to separate patients from controls. This may reflect that different patients with a similar disease have different metabolites perturbed in the same pathway, reflecting individual response to pathology. The decreased CSF levels of aminoadipic acid that we detect may indicate a decreased activity of the upstream enzyme aminoadipate aminotransferase, which also catalyzes the conversion of kynurenine to

kynurenic acid[53]. This is supported by our measurements of increases in the metabolites upstream of this enzyme in plasma, tryptophan and formylkynurenine; and reductions of this enzyme would shift this pathway towards the excitotoxic metabolite 3-hydroxykynurenine. Aminoadipic acid has previously been identified in an analysis from the longitudinal Framingham Heart Study as the single metabolite most significantly correlated to an increased risk for developing diabetes[54], which indicates an additional overlap between diabetes risk and neurodegenerative disease metabolic profiles.

In plasma from patients with ALS we also detected a significant decrease in asymmetric dimethylarginine (ADMA). An earlier report also detected reduced plasma concentration of ADMA in patients with ALS[55]. ADMA functions as an endogenous regulator of nitric oxide synthase[56] and consequently is involved in the synthesis of nitric oxide and the remediation of oxidative stress.

In this study we have validated several candidate metabolite biomarkers for PD. In patients with PD, alanine was increased in CSF and plasma. Alanine has previously been shown to be increased in CSF of PD patients[39, 57]. Alanine increases in PD CSF may indicate a disruption in the alanine/glucose shuttle, which is supported by alterations in plasma levels of α-ketoglutarate. Increased levels of ornithine in CSF in both ALS and PD may indicate a reduction in the ability of mitochondria to transport ornithine for conversion in the urea cycle. In plasma of patients with PD, we detected a significant increase in taurine relative to ALS and an increase relative to controls below significance threshold by univariate analysis (not shown). Taurine has previously been identified as increased in PD[58], and can be generated from cysteine upstream of glutathione synthesis.

Due to stringent requirements to reduce age span of patients and use the individually matched design to minimize the effect of metabolome variation in terms of sample age and gender effects, combined with the extensive range of metabolites measured, we anticipated significant false discovery rate. Nonetheless, we reported all detected significant alterations in metabolites between matched pairs, keeping this caveat in mind. To bring coherence to the metabolomics data and to compensate for the inherently high false discovery rates, we emphasize the value of external validation across studies. Metabolomics studies can further capture exogenous aspects of phenotype such as nutritional, environmental and pathogen derived changes that are beyond the scope of genomic or proteomic analysis. Due to the heterogeneous nature of neurodegenerative diseases, comparing different studies can be difficult and outcomes can be distorted by sub-groups of patients. Small sample sets will lack power to find significance of metabolites only altered in small subsets of patients and hence the false negative rate will be inherently high for such alterations. A limitation of this study is the fact that we did not include a group of healthy control samples that match rigorously to the ALS and PD samples. Instead we chose to represents patients with other diagnoses and differential diagnoses to ALS and/or PD that had visited our clinic for a lumbar puncture. Additional studies to identify subgroups of ALS and PD are warranted; and additional studies designed to distinguish neurodegenerative diseases from distinct medical conditions with compromised energy utilization such as diabetes mellitus are required to validate the clinical utility of many of the above metabolites in diagnostic biomarker panels.

Acknowledgements
We are indebted to the patients for their participation in this project. The sample preparation and mass spectrometry analysis was performed at the Swedish Metabolomics Center. The authors acknowledge Annika Johansson and Lina Mörén for help with the targeted amino acid analysis. This project has been generously supported by the Erling-Persson foundation, the Kempe foundation, the Swedish Medical Research Council, the Swedish Parkinson Disease Association and Ulla-Carin Lindquist foundation for ALS research.

Conflicts of interest
None of the authors report any conflicting interests.

Abbreviations

ADMA	Asymmetric dimethylarginine
ALS	Amyotrophic lateral sclerosis
AMP	Adenosine monophosphate
BCAA	Branched chain amino acids
CSF	Cerebrospinal fluid
DA	Discriminant analysis
EP	Effect projections
ESI +/−	Electrospray ionization, positive and negative mode
GC	Gas chromatography
LC	Liquid chromatography
MS	Mass spectrometry
mTORC1	Mechanistic target of rapamycin complex 1
OPLS	Orthogonal partial least squares projections to latent structures
PD	Parkinson's disease
%RSD	Relative standard deviation

Table 1. Number of Peaks and Metabolites Detected by the Analytical Platforms.

Analytical method	Biofluid	Number of peaks (%RSD*<40)	Number of identified unique metabolites (%RSD*<40)
Untargeted			
GC/MS	CSF	90**	52**
GC/MS	Plasma	103	50
LC/MS ESI+	CSF	261	42
LC/MS ESI+	Plasma	809	69
LC/MS ESI-	CSF	221	31
LC/MS ESI-	Plasma	290	104
Targeted			
LC/MS AccQ•Tag™	CSF	28	25
LC/MS AccQ•Tag™	Plasma	31	27
Total	CSF	600	144
Total	Plasma	1233	188

* %RSD is based on quality control samples measured across the analytical runs.

** Peaks from GC/MS for CSF were manually inspected for quality assessment due to missing quality control samples.

Table 2. Metabolites significant in ALS compared to matched controls and PD. The group showing increased metabolite level is listed.

Metabolite	Biofluid	HMDB	%RSD	Analysis	Control vs ALS	Control vs PD	ALS vs PD
α-hydroxybutate	CSF	HMDB00008	N/A	GC/MS	ALS	*n.s*	ALS
Carnitine	CSF	HMDB00062	5.12	LC/MS ESI+	ALS	*n.s*	ALS
Uracil	CSF	HMDB00300	N/A	GC/MS	Control	*n.s*	PD
Hypoxanthine	Plasma	HMDB00157	13.25	LC/MS ESI-	Control	*n.s*	PD

Table 3. Metabolites significant in ALS and PD compared to matched controls. The group showing increased metabolite level is listed.

Metabolite	Biofluid	HMDB	%RSD	Analysis	Control vs ALS	Control vs PD	ALS vs PD
Galactitol	CSF	HMDB00107	N/A	GC/MS	ALS	PD	*n.s*
Saccharic acid 1,4-lactone	CSF	N/A	N/A	GC/MS	ALS	PD	*n.s*
Ketoleucine	CSF	HMDB00695	8.53	LC/MS ESI-	ALS	PD	*n.s*
Ornithine	CSF	HMDB00214	4.85	LC/MS AA	ALS	PD	*n.s*
Sorbitol	CSF	HMDB00247	N/A	GC/MS	ALS	PD	*n.s*
Isoleucine	CSF	HMDB00172	4.19	LC/MS AA	ALS	PD	*n.s*
Indole	Plasma	HMDB00738	16.08	LC/MS ESI+	ALS	PD	*n.s*
Proline	Plasma	HMDB00162	7.03	GC/MS	ALS	PD	*n.s*

Figure legends

Figure 1. **Response of matched pairs in optimized OPLS-EP models.** Patients depicted as grey dots are labeled with the match number (listed in Table S1). Correlation of individual patients predicted profiles to the optimized OPLS-EP cross-validated models (Ypredcv) were plotted for CSF metabolites (x-axis) versus the predicted profiles using plasma metabolites (y-axis). A) Model of ALS versus matched control. B) Model of PD versus matched control. Y predicted=1 equals the model prediction of the disease, values greater than 1 represent a higher correlation to the disease profile in the OPLS-EP models and below one represent a lower correlation to the disease profile. Y predicted <0.5 indicates a patient that was not predicted to the disease group by the model. Y predicted <0 indicates a patient that was predicted similar to the matched control or opposite to the disease profile of the model.

Figure 2. **Metabolites significantly driving separation of ALS from matched controls in OPLS-EP models.** Model significant weights (w[1]) and univariate significant variables according to the univariate test are shown. The weight is the mean of the difference between ALS and matched control (of each metabolite). Value above zero means higher values in ALS and below zero means higher values in control. A) Model of ALS versus matched control in CSF. B) Model of ALS versus matched control in plasma.

Figure 3. **Metabolites significantly driving separation of PD from matched controls in OPLS-EP models.** Model significant weights (w[1]) and univariate significant variables according to the univariate test are shown. The weight is the mean of the difference between PD and matched control (of each metabolite). Value above zero means higher values in PD and below zero means higher values in control. A) Model of PD versus matched control in CSF. B) Model of PD versus matched control in plasma.

Figure 4. Metabolites significantly driving separation of ALS from matched PD in OPLS-EP models. Model significant weights (w[1]) and univariate significant variables according to the univariate test are shown. The weight is the mean of the difference between ALS and matched PD (of each metabolite). Value above zero means higher values in ALS and below zero means higher values in PD. A) Model of ALS versus matched PD in CSF. B) Model of ALS versus matched PD in plasma.

Figure 5. Sugar and ribonucleotide metabolism dissected by metabolomics in ALS. Overview of hexose derivatives relation to the pentose derivatives, purine and pyrimidine metabolites found to be significantly altered in ALS.

References

1 M.S. Petersen, S Bech, E. Nosova, J. Aasly and M.J. Farrer. *Mov. Disord.*, 2015, **30**, 538-44.

2 M.H.B. Huisman, S.W. de Jong, M.C. Verwijs, H.J. Schelhaas, A.J. van der Kooi, M. de Visser, J.H. Veldink and L.H. van den Berg. *Neurology*, 2011, **77**, 1363-1369.

3 P.M. Andersen and A. Al-Chalabi. *Nat. Rev. Neurol.,* 2011, **7**, 603-615.

4 S.C. Ling, M. Polymenidou and D.W. Cleveland. *Neuron,* 2013, **79**, 416-438.

5 H. Zhang, C. Duan and H. Yang. *Mol Neurobiol,* 2015, **51**, 89-104.

6 A.M. Gorman. *J. Cell. Mol. Med.*, 2008, **12**, 2263-2280.

7 A. Mehta, M. Prabhakar, P. Kumar, R. Deshmukh and P.L. Sharma*. Eur. J. Pharmacol.*, 2013, **698**, 6–18.

8 M. Vendruscolo, T.P.J. Knowles and C.M. Dobson. *Perspect. Biol*., 2011, **3**, pii: a010454.

9 R.A. Nixon. *Nat. Med.*, 2013, **19**, 983-997.

10 S. Rozen, M.E. Cudkowicz, M. Bogdanov, W.R. Matson, B.S. Kristal, C. Beecher, S. Harrison, P. Vouros, J. Flarakos, K. Vigneau-Callahan, T.D. Matson, K.M. Newhall, M.F. Beal, R.H. Brown Jr and R. Kaddurah-Daouk. *Metabolomics*, 2015, **1**, 101-108.

11 A. Nordström and R. Lewensohn. *J. Neuroimmune Pharmacol.*, 2010, **5**, 4-17.

12 J. Van der Greef, H. van Wietmarschen, B. van Ommen and E. Verheij. *Mass Spectrom. Rev*, 2013, **32**, 399-415.

13 E. Thysell, I. Surowiec, E. Hörnberg, S. Crnalic, A. Widmark, A.I. Johansson, P. Stattin, A. Bergh, T. Moritz, H. Antti and P. Wikström*. PLoS One*, 2010, **5**, e14175.

14 K. Dettmer, P.A. Aronov and B.D. Hammock. *Mass Spectrom. Rev.*, 2007, **26**, 51-78.

15 P. Jonsson, A. Wuolikainen, E. Thysell, E. Chorell, P. Stattin, P. Wikström and H. Antti*. Metabolomics,* 2015, **11**, 1667-1678.

16 Declaration of Helsinki World Medical Association. Available from: http://www.wma.net [accessed on 17 September 2015].

17 M. Otto, R. Bowser, M. Turner, J. Berry, J. Brettschneider, J. Connor, J. Costa, M. Cudkowicz, J. Glass, O. Jahn, S. Lehnert, A. Malaspina, L. Parnetti, A. Petzold, P. Shaw, A. Sherman, P. Steinacker, S. Süßmuth, C. Teunissen, H. Tumani, A. Wuolikainen and A. Ludolph. *Amyotrophic Lateral Scler*, 2012, **13**, 1-10.

18 A. Wuolikainen, M. Hedenström, T. Moritz, S.L. Marklund, H. Antti and P.M. Andersen. *Amyotrophic Lateral Scler.*, 2009, **10**, 229-U8.

19 EFNS Task Force on Diagnosis and Management of Amyotrophic Lateral Sclerosis, P.M. Andersen, S. Abrahams, G.D. Borasio, M. de Carvalho, A. Chio, P. Van Damme, O. Hardiman, K. Kollewe, K.E. Morrison, S. Petri, P.F. Pradat, V. Silani, B. Tomik, M. Wasner and M. Weber. *Eur. J. Neurol.*, 2012, **19**, 360-375.

20 J. A, J. Trygg, J. Gullberg, A.I. Johansson, P. Jonsson, H. Antti, S.L. Marklund and T. Moritz. *Anal. Chem.,* 2005, **77**, 8086-8094.

21 S. Wold, K. Esbensen and P. Geladi. *Chemom. Intell. Lab. Syst.*, 1987, **2**, 37-52.

22 J. Trygg and S. Wold. *J. Chemom*., 2002, **16**, 119-128.
23 M. Bylesjö, M. Rantalainen, O. Cloarec, J. Nicholson, E. Holmes and J. Trygg. *J. Chemom*., 2006, **20**, 341-351.
24 A. Wuolikainen, T. Moritz, S.L. Marklund, H. Antti and P.M. Andersen. *PLoS One*, 2011, **6**, e17947.
25 A. Wuolikainen, P.M. Andersen, T. Moritz, S.L. Marklund and H. Antti. *Mol. Genet. Metab*., 2012, **105**, 472-478.
26 E. Steen, B.M. Terry, E.J. Riviera, J.L. Cannon, T.R. Neely, R. Tavares, X.J. Xu, J.R. Wands and S.M. de la Monte. *J Alzheimer Dis*, 2005, **7**, 63-80.
27 P.F. Pradat, G. Bruneteau, P.H. Gordon, L. Dupuis, D. Bonnefont-Rousselot, D. Simon, F. Salachas, P. Corcia, V. Frochot, J.M. Lacorte, C. Jardel, C. Coussieu, N. Le Forestier, L. Lacomblez, J.P. Loeffler and V. Meininger. *Amyotrophic Lateral Scler*, 2010, **11**, 166-171.
28 L. Dunn, G.F. Allen, A. Mamais, H. Ling, A. Li, K.E. Duberley, I.P. Hargreaves, S. Pope, J.L. Holton, A. Lees, S.J. Heales and R. Bandopadhyay. *Neurobiol. Aging*, 2014, **35**, 1111-1115.
29 G.J. Biessels, S. Staekenborg, E. Brunner, C. Brayne and P. Scheltens. *Lancet Neurol.*, 2006, **5**, 64-74.
30 N.I. Bohnen, V. Kotagal, M.L. Müller, R.A. Koeppe, P.J. Scott, R.L. Albin, K.A. Frey and M. Petrou. *Parkinsonism Related Disorders*, 2014, **20**, 1394-1398.
31 I. Aviles-Olmos, J. Dickson and Z. Kefalopoulou. *J. Clin. Invest.,* 2013, **123**, 2730-2736.
32 J.C. Desport, F. Torny, M. Lacoste, P.M. Preux and P. Couratier. *Neurodegener. Dis.*, 2005, **2**, 202-207.
33 L. Dupuis, H. Oudart, F. René, J.L. Gonzalez de Aguilar and J.P. Loeffler. *Proc. Natl. Acad. Sci. U. S. A.*, 2004, **101**, 11159-11164.
34 B. Funalot, J.C. Desport, F. Sturtz, W. Camu and P. Couratier. *Amyotrophic Lateral Scler.*, 2009, **10**, 113-117.
35 E. Gray, J.R. Larkin, T.D. Claridge, K. Talbot, N.R. Sibson and M.R. Turner. *Amyotroph Lateral Scler Frontotemporal Degener*., 2015, **29**, 1-8.
36 W.E. Gall, K. Beebe, K.A. Lawton, K.P. Adam, M.W. Mitchell, P.J. Nakhle, J.A. Ryals, M.V. Milburn, M. Nannipieri, S. Camastra, A. Natali and E. Ferrannini; RISC Study Group. *PLoS One*, 2010, **5**, e10883.
37 P.J. Oates. *Int. Rev. Neurobiol*., 2002, **50**, 325-392.
38 C. Czech, P. Berndt, K. Busch, K. Busch, O. Schmitz, J. Wiemer, V. Most, H. Hampel, J. Kastler and H. Senn. *PLoS One*, 2012, **7**, e31501.
39 M. Trupp, P. Jonsson, A. Öhrfelt, H. Zetterberg, O. Obudulu, L. Malm, A. Wuolikainen, J. Linder, T. Moritz, K. Blennow, H. Antti and L. Forsgren. *J Parkinsons Dis*, 2014, **4**, 549-560.
40 K.A. Lawton, M.V. Brown, D. Alexander, Z. Li, J.E. Wulff, R. Lawson, M. Jaffa, M.V. Milburn, J.A. Ryals, R. Bowser, M.E. Cudkowicz and J.D. Berry; Northeast ALS Consortium. *Amyotrophic Lateral Scler. Frontotemporal Degener.*, 2014, **15**, 362-370.
41 L.D. Roberts, A. Koulman and J.L. Griffin. *Lancet Diabetes Endocrinol*, 2014,

2, 65-75.
42 H.J. Park, Y.B. Hong, Y.C. Choi, J. Lee, E. J. Kim, J.S. Lee, W. M. Mo, S. M. Ki, H.I. Kim, H.J. Kim, Y.S. Hyun, H.D. Hong, K. Nam, S. C. Jung, S.B. Kim, S.H. Kim, D.H. Kim, K.W: Oh, S.H. Kim, J.H. Yoo, J.E. Lee, K.W. Chung and B.O. Choi. *Ann Neurol*, 2015, doi: 10.1002/ana.24550. [Epub ahead of print].
43 J.R. Gooding, M.V. Jensen, X. Dai, B.R. Wenner, D. Lu, R. Arumugam, M. Ferdaoussi, P.E. MacDonald and C.B. Newgard. *Cell Rep,* 2015, **13**, 157-67.
44 J.M. Shefner, M.E. Cudkowicz, D. Schoenfeld, T. Conrad, J. Taft, M. Chilton, L. Urbinelli, M. Qureshi, H. Zhang, A. Pestronk, J. Caress, P. Donofrio, E. Sorenson, W. Bradley, C. Lomen-Hoerth, E. Pioro, K. Rezania, M. Ross, R. Pascuzzi, T. Heiman-Patterson, R. Tandan, H. Mitsumoto, J. Rothstein, T. Smith-Palmer, D. MacDonald and D. Burke; NEALS Consortium. *Neurology,* 2004, **63**, 1656-1661.
45 H. Blasco, L. Nadal-Desbarats, P.F. Pradat, P.H. Gordon, C. Antar, C. Veyrat-Durebex, C. Moreau, D. Devos, S. Mavel, P. Emond, C.R. Andres and P. Corcia. *Neurology*, 2014, **82**, 1167-1174.
46 K. Kanamori, B.D. Ross and R.W. Kondrat. *J. Neurochem.*, 1998, **70**, 1304-1315.
47 J.L. Jewell, Y.C. Kim, R. Russel, F-X. Yu, H.W. Park, S.W. Plouffe, V.S. Tagliabracci and K.L. Guan. *Science,* 2015, **347**, 194-198.
48 J. Averous, S. Lambert-Langlais, V. Carraro, O. Gourbeyre, L. Parry, W. B'Chir, Y. Muranishi, C. Jousse, A. Bruhat, A.C. Maurin, C.G. Proud and P. Fafournoux. *Cell Signal,* 2014, **26**, 1918-1927.
49 P.A Lewitt, J. Li, M. Lu, T.G. Beach, C.H. Adler and L. Guo; Arizona Parkinson's Disease Consortium. *Mov. Disord.*, 2013, **28**, 1653-1660.
50 L. Tan, J.T. Yu and L. Tan. *J. Neurol. Sci.*, 2012, **323**, 1–8.
51 Ogawa T, Matson WR, Beal MF, Myers RH, Bird ED, Milbury P and Saso S. *Neurology*, 1992, **42**, 1702-1706.
52 G. Oxenkrug. *Mol. Neurobiol*., 2013, **48**, 294–301.
53 Q. Han, T. Cai, D.A. Tagle, H. Robinson and J. Li. *Biosci Rep*, 2008, **28**,205-15.
54 T.J. Wang, D. Ngo, N. Psychogios, A. Dejam, M.G. Larson, R.S. Vasan, A. Ghorbani, J. O'Sullivan, S. Cheng, E.P. Rhee, S. Sinha, E. McCabe, C.S. Fox, C.J. O'Donnell, J.E. Ho, J.C. Florez, M. Magnusson, K.A. Pierce, A.L. Souza, Y. Yu, C. Carter, P.E. Light, O. Melander, C.B. Clish and R.E. Gerszten. *J Clin Invest,* 2013, **123**, 4309-4317.
55 C. Isobe, T. Abe and Y. Terayama. *Neurosignals*., 2010, **18**, 43-48.

56 P. Vallance and J. Leiper. *Arterioscler., Thromb., Vasc. Biol.*, 2004, **24**, 1023-1030.
57 K. Araki, T. Takino, S. Ida and K. Kuriyama. *Acta. Neurol. Scand.*, 1986, **73**, 105-110.
58 J.A. Molina, F.J. Jimenez-Jimenez, P. Gomez, C. Vargas, J.A. Navarro, M. Ortí-Pareja, T. Gasalla, J. Benito-León, F. Bermejo and J. Arenas. *J. Neurol. Sci*, 1997, **150**, 123-127.

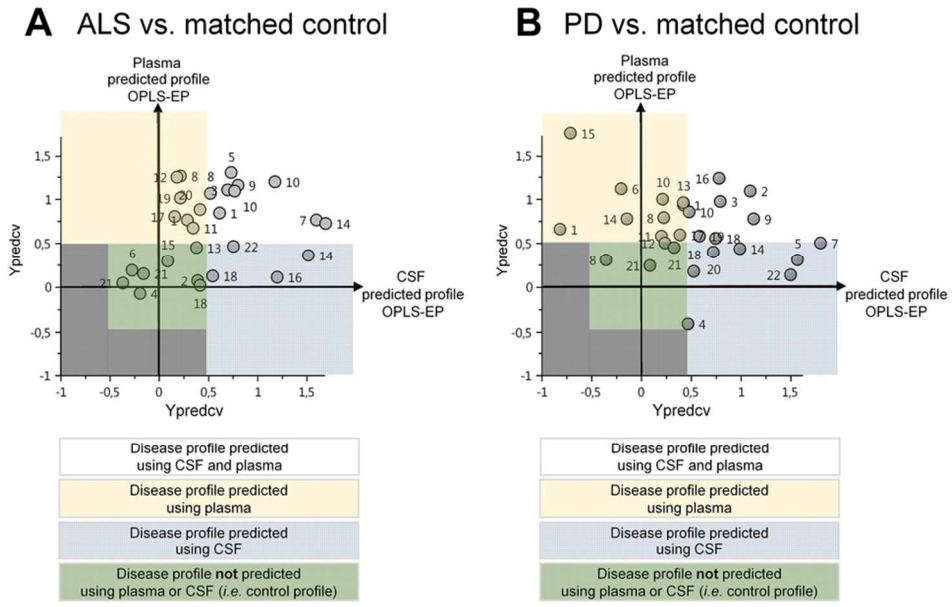

86x56mm (300 x 300 DPI)

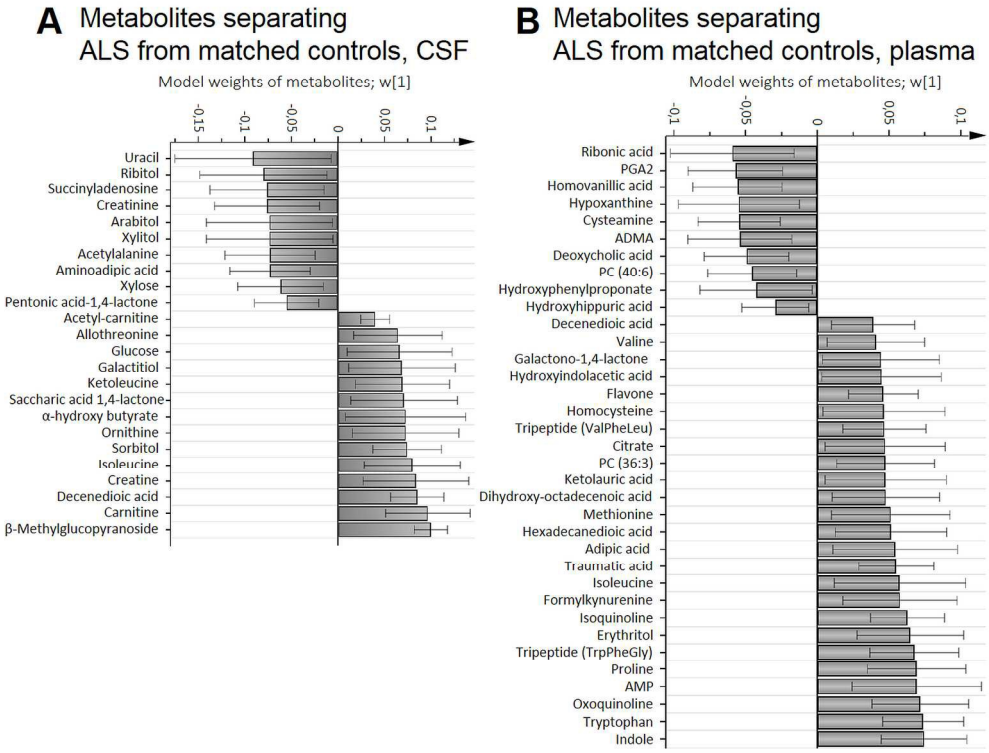

181x139mm (300 x 300 DPI)

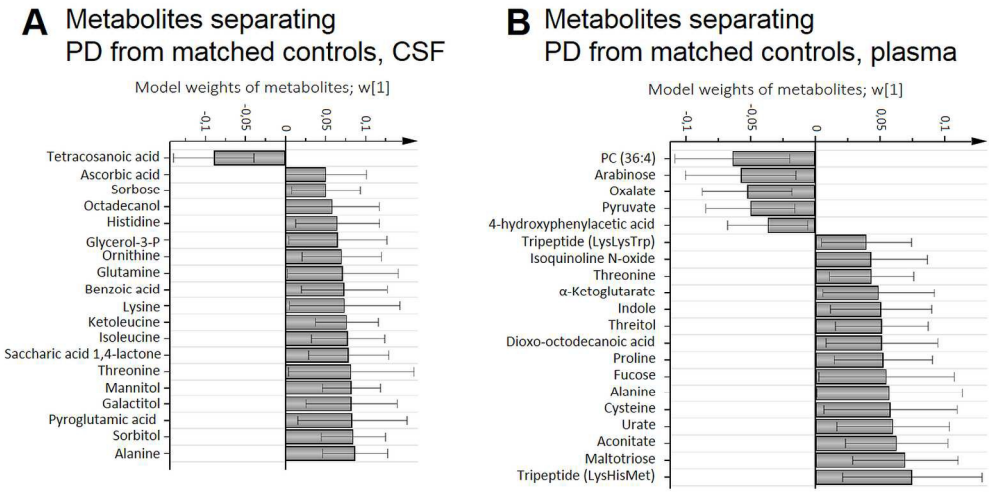

181x91mm (300 x 300 DPI)

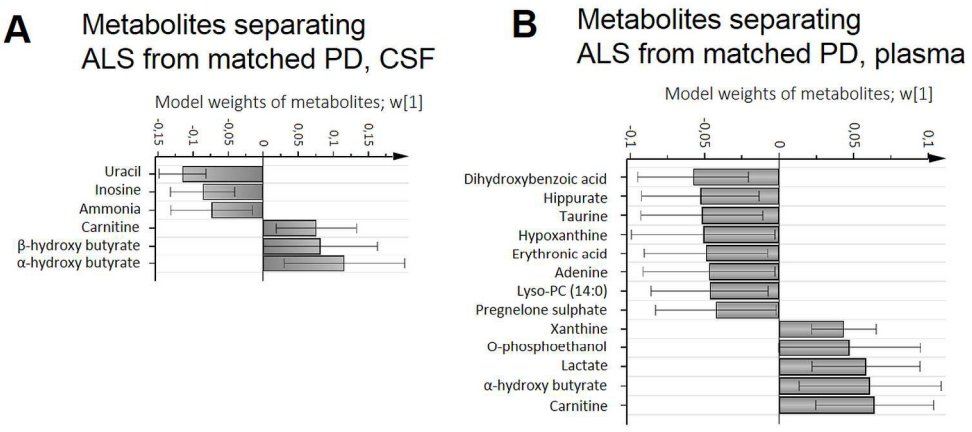

181x80mm (300 x 300 DPI)

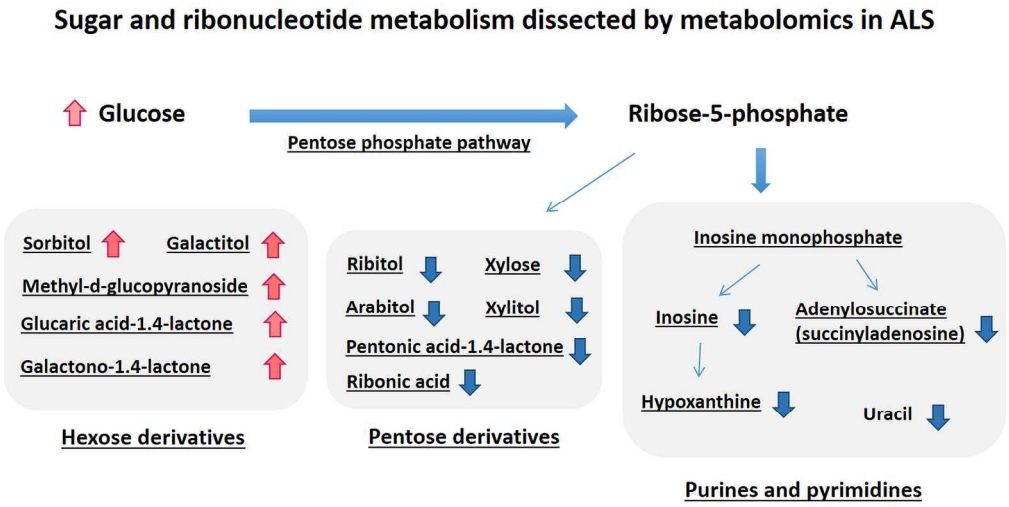

181x94mm (300 x 300 DPI)